Journal of Catalysis 429 (2024) 115215

Contents lists available at ScienceDirect

Journal of Catalysis

journal homepage: www.elsevier.com/locate/jcat

Increasing the HER efficiency of photodeposited metal nanoparticles over TiO_2 using controlled periodic illumination

Fabrizio Sordello [a], Marco Prozzi [a], Vasile-Dan Hodoroaba [b], Jörg Radnik [b], Francesco Pellegrino [a,c,*]

[a] Department of Chemistry and NIS Centre, University of Torino, Via Giuria 7, 10125 Torino, Italy
[b] Federal Institute for Materials Research and Testing (BAM), Unter den Eichen 44-46, 12203 Berlin, Germany
[c] UniTo-ITT JointLab, University of Torino, Via Quarello 15/A, 10135 Torino, Italy

ARTICLE INFO

Keywords:
Controlled periodic illumination
Hydrogen evolution reaction
Titanium dioxide
Photoreforming
Volcano plot
Sabatier
Nanoparticles

ABSTRACT

Although the use of noble metal catalysts can increase the efficiency of hydrogen evolution reaction, the process is still limited by the characteristics of the metal-hydrogen (M−H) bond, which can be too strong or too weak, depending on the metal employed. Studies revealed that the hydrogen affinity for the metal surface (i.e. H absorption/desorption) is regulated also by the potential at the metal nanoparticles. Through controlled periodic illumination (CPI) of a series of metal/TiO_2 suspensions, here we demonstrated that an increase of the HER efficiency is possible for those photodeposited metals which have a Tafel slope below 125 mV. Two possible explanations are here reported, in both of them the M−H interaction and the metal covering level play a prominent role, which also depend on the prevailing HER mechanism (Volmer-Heyrovsky or Volmer-Tafel).

1. Introduction

The global primary energy consumption has increased steadily since industrial revolution due to the growth of the population and the progress of the people lifestyle, in both developed and developing countries.[1,2] Obviously, the increase of the consumption has gone hand in hand with the rise in the use of fossil fuels and, therefore, of CO_2 emissions.[3] The abatement of CO_2 emissions is a fundamental aspect for coping with climate change, one of the most important challenges for humanity in the next decades,[4,5] as acknowledged and summarized by Rockström et al. in their definition of planet boundaries.[6] Among the most promising technologies, green hydrogen (H_2) production is the most relied-upon. It will be developed and used for the production of energy in a less impactful way.[7,8] In this context, direct conversion of light into chemicals through water photosplitting using semiconductor photocatalysts (such as TiO_2) has been considered a sustainable method to produce clean fuel.[9,10] Water splitting can be considered as the sum of two different reactions: hydrogen evolution reaction (HER) and oxygen evolution reaction (OER). Both of them still have problems of efficiency, although extensive research efforts have been carried out in the last decades.[11] The best strategy employed until now to increase the HER rates is the use of noble metals (Pt, Pd, Rh, etc.) as co-catalyst.[12] The metals deposited at the interface of the semiconductor (typically TiO_2) are able to extract the photogenerated electrons from it, suppressing charge carrier recombination and increasing the kinetic transfer to protons and water.[10,13] The drawbacks of these noble metals are, of course, the costs, which reflect their limited abundance on Earth's crust. For this reason, in the last years, several researchers focused their attention on the replacement of these noble metals with less expensive substitutes or on the optimization in term of efficiency of such kind of metal–semiconductor systems.[11].

In our latest work on this topic, we developed a strategy for increasing the quantum yield of the HER over Pt-TiO_2 nanoparticles in suspension, employing controlled periodic illumination (CPI).[14] In the CPI, the incident photonic flux on the reaction cell is modulated over time according to a square wave: this consists of an alternate repetition of light time (t_{ON}) and dark time (t_{OFF}). The light source modulation is characterized by two parameters: the duty cycle ($\gamma = t_{ON}/(t_{ON} + t_{OFF})$ and the frequency of the square wave.[15] In our work published in 2021, [14] we observed an increase of the HER efficiency using CPI at different frequencies (0.8, 80 and 8000 Hz) in comparison to the continuous illumination.[14] The mechanism responsible for the increase of the HER rates was at that time not fully understood. It seems that, during CPI, there is a change of the charge carrier dynamics, which

* Corresponding author.
E-mail address: francesco.pellegrino@unito.it (F. Pellegrino).

https://doi.org/10.1016/j.jcat.2023.115215
Received 14 June 2023; Received in revised form 2 November 2023; Accepted 19 November 2023
Available online 23 November 2023

leads to a better separation and decreased recombination of electrons and holes. Those results were particularly important considering that it was the first time where CPI was demonstrated to be advantageous compared with standard continuous irradiation with the same energy input. The significance of such a result motivated us to further investigate the mechanism to better understand the phenomenon, and hence possibly further increase the efficiency gains.

Therefore, the objective of the present work was to evaluate the effect of different metals photodeposited on bipyramidal TiO_2 nanoparticles in the HER under CPI. The deposition methods of a metal on titanium dioxide can be different, in our case we focused on photodeposition always using the same procedure protocol but varying the precursor of the metal to be deposited. Together with advanced methods for the characterization of the materials, we also tried to elucidate the mechanism through electrochemical experiments on a vaster collection of materials to discriminate among various hypotheses made in the previous paper.

2. Experimental

2.1. TiO_2 bipyramidal synthesis

Our group already reported the material synthesis in several other papers.[10] Briefly, the nanoparticles were obtained by forcing the hydrolysis of a 40 mM aqueous solution of $Ti(TeoaH)_2$ complex (TeoaH = triethanolamine; initial pH 10), carried out through hydrothermal treatment at 493 K for 50 h in autoclave. The material was then heated at 873 K for 1 h in air atmosphere. This material exposes nearly 90 % of the reductive surfaces [1 0 1].[10].

2.2. Metal photodeposition and photocatalytic experiments

The deposition of the different metals over the TiO_2 bipyramidal nanoparticles was carried out through photodeposition, irradiating with UV light (45 min) slurries containing 1.0 g/L of TiO_2 and 2.0 mg/L of the metal ion. The metal is reduced during irradiation to the zero-valent metallic form (by the photoelectrons produced in the semiconductor) and deposited onto TiO_2 upon irradiation. The metal precursors employed (all purchased from Merck) were: 1.00 mg/mL of Pt in 5 % HCl standard solution, 1.01 mg/mL of Rh in 5 % HCl standard solution, 1.01 mg/mL of Pd in 5 % HCl standard solution, $HAuCl_4$, $AgNO_3$, $CuCl_2$. The experiments were carried out at pH 2.4 using formic acid 0.1 M (that is also the hole scavenger). The irradiations were carried out in magnetically stirred, cylindrical quartz cells, containing 100 mL of slurry (therefore 100 mg of material). Before irradiation, the cell containing the slurry was carefully purged with nitrogen to remove oxygen from the reaction environment. The removal of oxygen is fundamental in order to avoid the competitive oxygen reduction reaction. Hydrogen production experiments were performed irradiating the previously prepared suspension (after 15 min of sonication) with UV light.

Hydrogen evolution was followed sampling periodically 2.5 mL of gas from the irradiation cell and replacing it with the same volume of N_2. The HER was carried out using 0.1 M of formic acid as hole scavenger. The gas sample was analyzed with an Agilent 490 Micro GC gas chromatograph equipped with a Molsieve 5Å column for H_2 analysis and a Poraplot U column for CO_2 quantitation. During the analysis, the columns were kept at temperatures of 363 K and 313 K at a pressure of 200 kPa and 150 kPa, respectively. The carrier gases were argon and helium, respectively. The total amounts of H_2 produced as a function of time were calculated from the concentration in the sampled gas, considering the total volume of gas in the irradiation cell and the previous samplings. The irradiation was carried out with a LED source centered at 365 nm. The irradiation system and conditions are fully described in our previous papers.[14,15].

2.3. Photoelectrochemical characterization

The photoelectrochemical characterization was carried out on TiO_2 electrodes produced by dropping 1.0 mL of the TiO_2 or Me-TiO_2 suspension over a fluorine doped tin oxide (FTO) glass and subsequent drying in air at room temperature. The illuminated area of the electrodes is nearly 6 cm^2. The electrochemical measurements were performed using a standard photo-electrochemical setup, composed of a computer-controlled potentiostat, AUTOLAB PGSTAT12, and the same light source employed for the H_2 evolution experiments. The electrochemical cell was a conventional three-electrode cell with a 1 mm thick fused silica window. The counter and reference electrodes were a glassy carbon and an Ag/AgCl/KCl (3 M) electrode, respectively. Electrochemical Impedance Spectroscopy (EIS), Linear Sweep Voltammetry (LSV), open circuit potential (OCP) and chronoamperometric (CA) measurements were carried out under a N_2 atmosphere (flux 200 mL min^{-1}); the solution (0.1 M formic acid) was purged with N_2 for 30 min before each measurement in order to eliminate the residual O_2 present in the solution, to obtain the recombination rate of the photogenerated carriers. The experiments are carried out at pH 2.4 to reproduce the same experimental conditions adopted during photocatalytic hydrogen evolution. Scan rate for the LSV was 0.005 V s^{-1}. The potential bias employed for CA measurements was 0 V (vs Ag/AgCl) to minimize the dark current. EIS characterization was carried out in the dark, under continuous irradiation and under CPI. All measurements were carried out at the OCP, sampling 50 frequency values between 10 kHz and 100 mHz. Measurements were repeated to verify the stability of the materials under measuring conditions. The electrochemical tests were not carried out for Cu-TiO_2 because in the employed conditions the Cu nanoparticles were not stable, as they dissolved due to the acidic pH. Nevertheless, photocatalytic experiments were possible, because our procedure allowed the deposition of Cu particles under irradiation and the subsequent assessment of HER rate without interrupting the irradiation and, therefore, maintaining conditions at which it was possible to have a certain amount of reduced Cu on the material, even though in dynamic equilibrium with its oxidized soluble species.

2.4. XPS characterization

The samples were measured as powders fixed on a double-adhesive tape on a stainless steel sample holder. The XPS measurements were conducted with an AXIS Ultra DLD photoelectron spectrometer (Kratos Analytical, Manchester, UK) with monochromatic Al Kα radiation ($h\nu$ = 1486.6 eV) at a pressure of approximately 5×10^{-9} mbar. The electron emission angle was 0° and the source-to-analyzer angle was 60°. The binding energy scale of the instrument was calibrated following a Kratos Analytical procedure which uses ISO 15472 binding energy data.[16] The XPS spectra were recorded in the fixed analyzer transmission (FAT) mode, in the hybrid lens mode and the slot mode providing approximately a 300×700 μm^2 analysis area, using a charge neutralizer. Survey spectra were measured with a pass energy of 80 eV; high-resolution spectra were recorded with a pass energy of 20 eV. The survey spectra were used for element identification. For the determination of the valence states, the high-resolution spectra were fitted with the sum of a Gaussian-Lorentzian curve. For the background of the peaks a modified Tougaard background was used.[17] The uncertainty of the electron binding energy is estimated within ± 0.2 eV.

2.5. Electron microscopy characterization

The SEM used is of type Zeiss Supra 40 (Zeiss, Oberkochen, Germany) being equipped with a Schottky field emitter and a secondary electron (SE) InLens detector additionally to the conventional SE (Everhart-Thornley) one. The attained resolution is of a few nm. Energy-dispersive X-ray spectroscopy (EDS) has been carried out with the attached silicon drift detector (SDD) spectrometer of type Thermo

UltraDry (Thermo Scientific, Waltham. MA, USA) having a nominal area of the silicon sensor of 100 mm^2, i.e. a spectrometer of high sensitivity regarding detection of X-ray signals from individual nanoobjects. The spectra have been taken and analysed with the Thermo software Pathfinder 1.3.

3. Results and discussion

Taking inspiration from the previous work,[14] we carried out HER on metal/TiO_2 slurries modulating the square wave incident UV irradiation at 80 Hz with a fixed duty cycle of 0.2. This frequency was chosen because of the good results obtained in terms of performance improvement switching from continuous illumination to CPI in our previous work.

In Fig. 1 we report the trends of the hydrogen evolution rate under continuous illumination (black curves) and CPI at 80 Hz (red curves) for the six materials considered.

Hydrogen evolution is significantly larger under CPI compared with the continuous illumination in the presence of Pt (+32 %), Rh (+36 %) and Pd (+22 %). While for Au, Cu and Ag there is no significant difference between CPI and continuous illumination in the conditions here employed for the photocatalytic tests (the differences are in the limit of the experimental error for such kind of experiments).

However, It must be underlined that the interaction of hydrogen with the surface of the metals may depend on several factors, such as oxidation state, environment conditions and morphology of the nanoparticles. For this reason, in Supplementary Material (SM) I we report the detailed XPS and SEM/EDS analysis results of all the materials synthetized and tested. SEM/EDS results indicate that during the irradiation every precursor is reduced at the surface of the TiO_2 producing nanoparticles with different morphology and composition. These results lead to the conclusion that the size of the nanoparticles does not influence the catalytic activity under CPI. For example, Rh and Au nanoparticles photodeposited over TiO_2 have similar size (nearly 20–30 nm), but a completely different behavior. However, size is not the only factor that can determine the photocatalytic activity of a catalyst. XPS analysis highlights the incomplete chemical homogeneity of the nanoparticles reduced at the surface of the titanium dioxide during photodeposition. A pure metallic form or a mixture of metal and metal oxide can compose them. However, the limit of such an analysis is the time elapsed between synthesis and characterization, during which the oxidation of the metal can occur. To further investigate the role of the metallic co-catalyst, HER was monitored in the presence of different nominal amounts of Pt (see SI Figure S14). It is possible to observe that there is a linear increase of the percentage increment of the photocatalytic activity under CPI vs. continuous irradiation (and therefore of the quantum yield of the reaction) with the amount of Pt. Therefore, increasing the surface concentration of the co-catalyst makes it possible to enhance the CPI effect on the system. This effect is completely unrelated to the reaction rate, which is maximized at lower (0.2 %) to intermediate (0.8 %) Pt loadings. The linear dependence confirms the hypothesis that the reaction can be closely linked to the presence of a metal co-catalyst and, therefore, to the adsorption/desorption mechanism of hydrogen from its surface even more consistently.

Electrochemical characterization was carried out to better understand the mechanisms beyond the CPI. First, it is interesting to note that the CPI influences all the materials, including those that do not show an increase of the efficiency. This can be observed with open circuit potential (OCP) and chronoamperometry (CA) measurements reported in Fig. 2 for the Pd-TiO_2 and Au-TiO_2 cases. As already observed in the previous work for pristine TiO_2, also in these cases during the CPI the potential measured during OCP drops a few mV and the photocurrent revealed by CA grows. The same occurs for all the other materials analyzed (see SM). This means that CPI is able to affect the charge carriers' kinetics in all the materials, increasing their lifetime and density under irradiation. However, only those with peculiar characteristics did reach a significant improvement of the reaction rate.

EIS evidenced great differences among dark and irradiation experiments, due to the improved charge transfer to solution, i.e. electron transfer from the materials to protons to give HER (Fig. 3). While in the dark larger impedance values are recorded, under irradiation the Nyquist plots closely resemble half circles, whose diameter gives and estimation of the charge transfer resistance: the lower the resistance the more efficient HER becomes.

Comparing now continuous irradiation with the CPI experiments much smaller differences can be observed. In both cases Nyquist plots are half circles, and for all the materials tested the diameter is significantly smaller under CPI, i.e. lower charge transfer resistance, witnessing improved charge transfer under CPI compared with continuous irradiation, especially for the Au, Ag and bare TiO_2. Again, this finding is

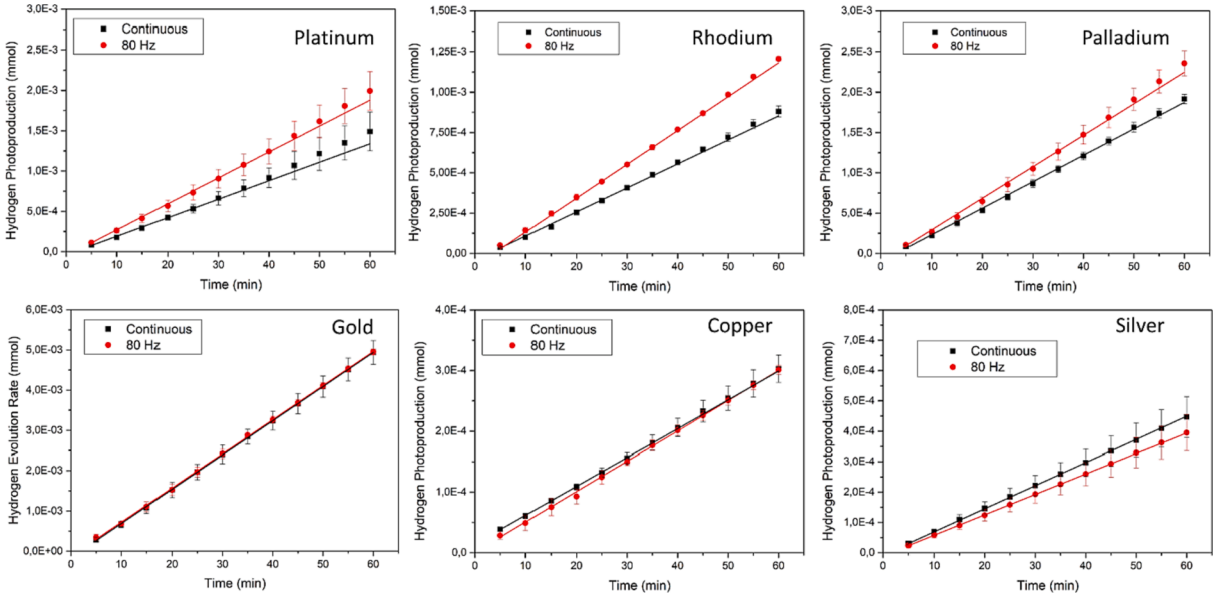

Fig. 1. Trends of the hydrogen photoproduction under continuous illumination (black lines) and CPI at 80 Hz (red lines) for the six materials considered. (For interpretation of the references to colour in this figure legend, the reader is referred to the web version of this article.)

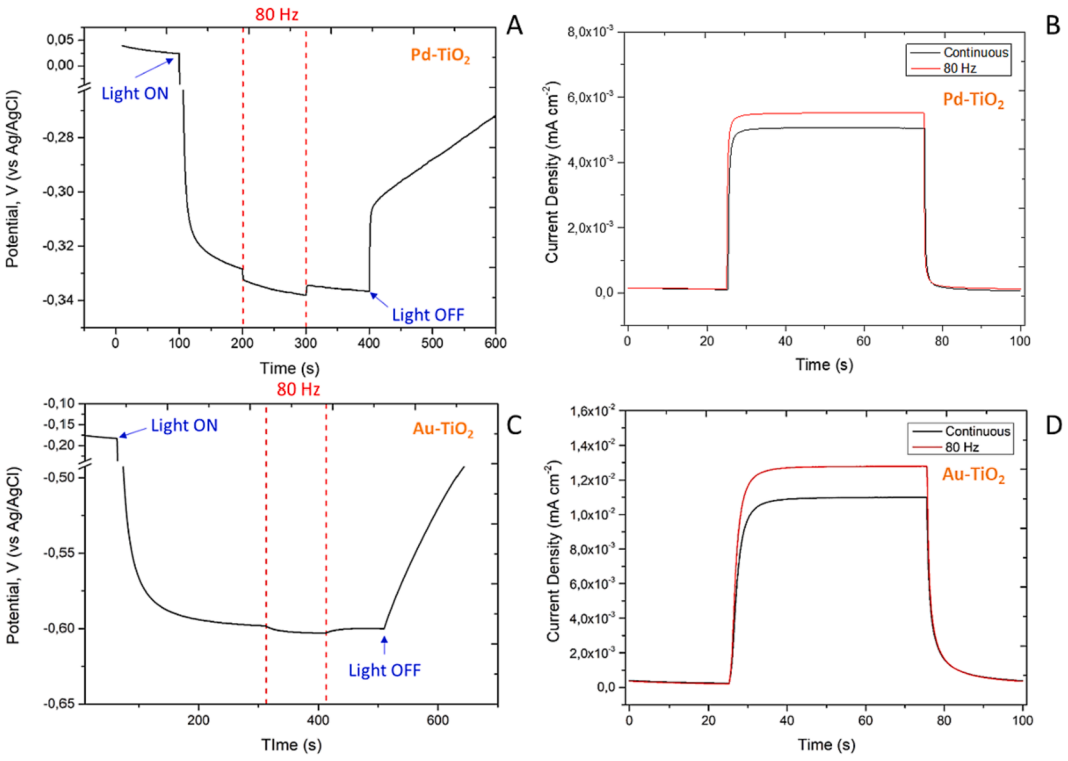

Fig. 2. OCP (A and C) and CA (B and D) analysis for the catalyst Pd-TiO_2 (top) and Au-TiO_2 (bottom).

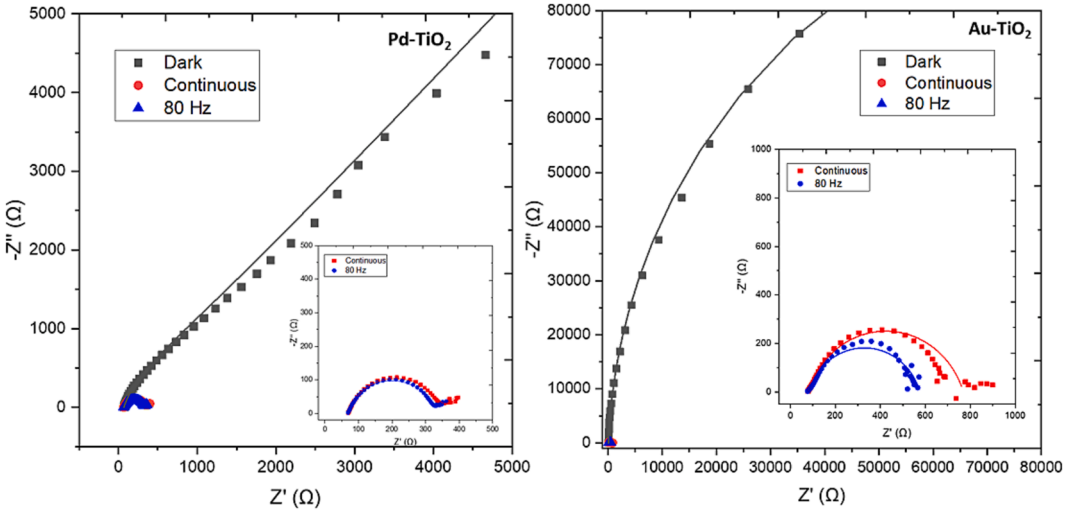

Fig. 3. EIS analysis of Pd-TiO_2 (left) and Au-TiO_2 (right) materials.

in very good accordance with OCP monitoring, and CA, where we also observed better performance under CPI (larger photo-potentials in OCP and larger photocurrents in CA) for all the materials considered. The quantitative EIS analysis (Nyquist plot and the equivalent circuits employed for fitting) of all the materials is reported in the SM. However not all the materials are capable of converting these improved charge carrier dynamics into measurabily HER improvements.

In our previous work of 2021,[14] we hypothesized that the effectiveness of the CPI in the case of Pt-TiO_2 nanoparticles could be ascribed to the lower value of the Tafel slope for this material compared with bare TiO_2. The small decrease of the potential revealed with OCP (due to the larger charge carrier density) is relevant in the case of Pt-TiO_2 because of its relatively small Tafel slope, i.e. 30 mV (literature)[18] and 88 mV (this work, considering Pt-TiO_2), while the same change in the potential has a much lower effect on the bare TiO_2 catalyst, that presents high values of Tafel slope, i.e. 256 mV. In SM are reported the OCP and CA measurements for the other materials. To support our hypothesis, we carried linear sweep voltammetry (LSV) (see Fig. 4A) tests using electrodes obtained in accordance with the procedure described in the Experimental section. As highlighted in Fig. 4A, the cathodic offset is very different from metal to metal. The best performance is given by Pt-TiO_2 (as expected). Rh and Pd behave similarly, although Pd seems to reach higher current values. Ag and Au have an almost overlapping path, while bare TiO_2 is the least active catalyst. From the LSVs, we calculated the Tafel slopes as reported in Fig. 4B. The results confirm the existence of two distinct clusters. The three metals with low Tafel slopes, i.e. Pt, Rh and Pd, are the most affected by the CPI, as already observed in Fig. 1. At the same time, Au, Ag and bare TiO_2, which do not show

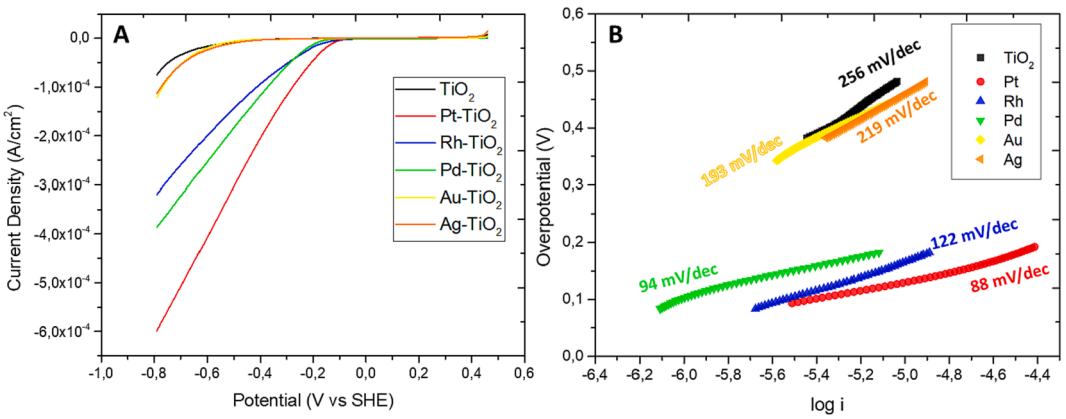

Fig. 4. Linear Sweep Voltammetry curves (A) and Tafel Slopes (B) for the materials employed in the work.

significant improvements under CPI, present ≈ 2.5-fold increase in the values of their Tafel slopes. It must be underlined that Tafel slopes here experimentally obtained are referred not to the bare metals, but to the combined metal–semiconductor. However, since the TiO_2 support is always the same and the HER mainly occurs at the metals' surfaces, the changes of the slopes can be attributed to the differences of the metals deposited.

Interestingly, the metals employed as co-catalysts are located in two different positions of the Volcano Plot for HER, as reported in Fig. 5B. Pt, Rh and Pd present the best catalytic activity, as they are close to the top of the "volcano" (in green) (n.b. in the original Trasatti's plot the presence of Pd is not reported, however several studies report characteristics similar to Pt and Rh).[19–21] In this region, the bond energy between the metal surface and the H atom absorbed is not too weak neither too strong, resulting in optimal adsorption–desorption rates. With these metals the reaction mechanism is slightly limited by the molecular hydrogen desorption (green zone in Fig. 5A). Further, the other three metals (Cu, Ag, and Au) present a reaction rate limited by reactant activation (blue zone in Fig. 5B), corresponding to weaker than optimal M−H bond strength.[19].

The same clustering of metal co-catalysts can be found with EIS Fig. 3 and Figure S5 in SM). Taking a closer look to charge transfer resistances, we found very good agreement with LSV results. Indeed, the values of charge transfer resistance can be divided into two groups of materials: Pd, Rh and Pt where it stays at roughly 300 Ω and Au, Ag and pristine TiO_2 where it ranges from 600 to 700 Ω. This division, again, corresponds with the grouping of metals based on their positioning on the Volcano plot for HER.

These results highlight that CPI seems to be able to act as a rate booster only in the presence of specific metals and the mechanism seems to be related to the absorption/desorption of H_2 from the surface of the metal catalyst. A first possible explanation is the "catalytic resonance" paradigm developed by Dauenhauer and coworkers.[23,24] In their work of 2020,[23] they modulated CO coverage at the Pt surface using pulsed illumination. This occurred because under illumination the effective CO binding energy on Pt is decreased compared with the binding energy in the dark, this resulting in the decrease of the CO coverage and the shift of the Pt to the weak binding side of the methanol decomposition activity volcano. This oscillation between strong binding during dark time and weak binding under light time is able to intermittently switch the rate limiting step and, consequently, allow the dynamic raise of the methanol decomposition rate.[23] In our case, we have an opposite situation: during the illumination time, the H_2 binding with the metal surface is higher compared to the dark time, because of the lower potential reached during irradiation. Therefore, during the dark time we have the removal of the H_2 from the surface, resulting in a higher number of active sites available for new reactions at the subsequent light period, and eventually improving the electron scavenging through proton reduction. Overall, this results in the reduced charge carriers' recombination observed in the electrochemical experiments. However, since the sensitivity of the system to the variation of the potential given by CPI is different for the various metals (as confirmed by the Tafel slope measured), the increase of the H_2 photoproduction cannot be observed in all the systems at the conditions employed here.

The second possible hypothesis is based on the reaction mechanisms in the production of H_2 at the surface of metals. In fact, for the HER

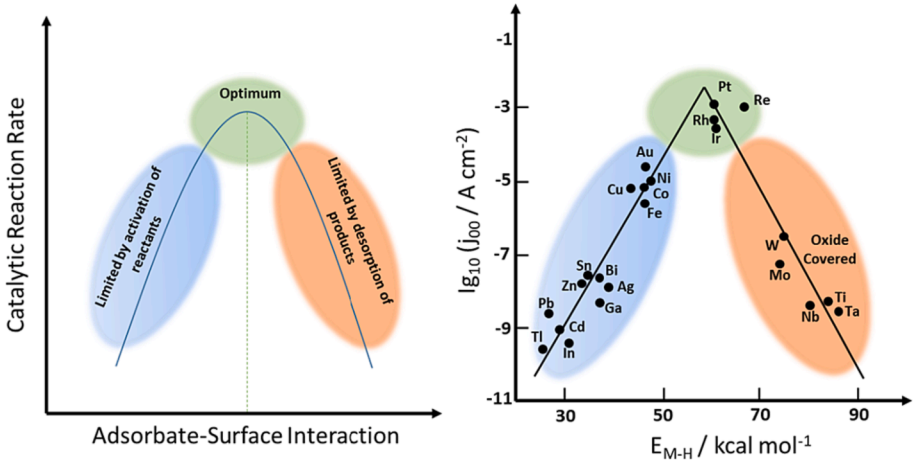

Fig. 5. Representation of the Volcano Plot (left) and Trasatti's plot for HER in acidic solutions (right)[19,22].

under acidic conditions, two different mechanisms occur on depending of metal characteristics: Volmer-Tafel or Volmer-Heyrovsky.[25–28] In both mechanisms, the first step involves the H^+ reduction and is called "Volmer" reaction:

$M + H^+ + e^- \rightarrow M{-}H$ (Volmer Reaction)

Once an adsorbed hydrogen atom (M−H) is present on the surface of the catalyst, it is possible to follow two different pathways:

1) reaction with another adsorbed hydrogen atom in a Langmuir-Hinshelwood type mechanism:

$2(M{-}H) \rightarrow 2\ M + H_2\ (g) \rightarrow \rightarrow$ (Tafel Reaction)

2) reaction with a solvated proton and a new electron with a Eley-Rideal mechanism:

$M{-}H + H^+ + e^- \rightarrow M + H_2\ (g) \rightarrow$ (Heyrovsky Reaction)

The main difference between the two reactions is that the Tafel reaction does not involve electron transfer while the Heyrovsky reaction does. Therefore, an applied voltage can modify the Heyrovsky path while the Tafel step is independent on applied potential.[25,28].

From literature, we know that metals like Ag and Au follow the Heyrovsky reaction, while metals such as Pt, Pd and Rh the Tafel one.[29] Considering that during CPI we alternate dark time and light time, and that the Tafel reaction does not require a second electron transfer, the Tafel reaction can occur even in the dark, provided that the previous light period produces a substantial hydride coverage on the metal co-catalyst, leading to H_2 generation also during dark periods. Moreover, on the subsequent light period photoelectrons can be scavenged by the metal co-catalyst more efficiently, as the metal surface has lower hydride coverage. On the other hand, the Heyrovsky reaction requires the production of two electrons consecutively, therefore during the dark time the catalyst cannot work, as photoelectron generation on the semiconductor stops. In this latter case, the overall picture resembles very much the photocatalytic oxidation of HCOOH on pristine TiO_2, where no effect of CPI was observed, because of the impossibility to effectively carry out the reaction in the dark [15].

4. Conclusions

We demonstrated that controlled periodic illumination (CPI) seems to be a valuable tool for enhancing the HER rate for those metals that present a low value of the Tafel slope. The latter is related to the kinetics and the mechanism of the HER. In particular, although CPI is able to influence the dynamics of the photogenerated charge carriers for all the materials here employed, as observed in all the electrochemical experiments carried out, the increase of the photocatalytic activity (and of the quantum yield) can be observed only in Pt, Pd and Rh. These metals have a limitation due to the H_2 desorption from the surface of the catalyst because of the strong M−H bond. CPI could induce a decrease of the M−H bond energy favoring the H_2 desorption. Moreover, these metals undergo a Volmer-Tafel mechanism, having the possibility of working in both light and dark times. These new findings certainly contributed to understand even more the effects of modulated lighting for the photocatalytic production of hydrogen on metal/semiconductor systems.

Declaration of Competing Interest

The authors declare that they have no known competing financial interests or personal relationships that could have appeared to influence the work reported in this paper.

Data availability

Data will be made available on request.

Acknowledgements

This publication is part of the project NODES which has received funding from the MUR – M4C2 1.5 of PNRR funded by the European Union - NextGenerationEU (Grant agreement no. ECS00000036).

Appendix A. Supplementary material

Supplementary data to this article can be found online at https://doi.org/10.1016/j.jcat.2023.115215.

References

[1] N. Armaroli, V. Balzani, The future of energy supply: Challenges and opportunities, Angew Chem Int Ed Engl 46 (2007) 52–66.
[2] C.D. Thomas, Climate, climate change and range boundaries, Divers. Distrib. 16 (2010) 488–495.
[3] P. Friedlingstein, R.A. Houghton, G. Marland, J. Hackler, T.A. Boden, T.J. Conway, J.G. Canadell, M.R. Raupach, P. Ciais, C. Le Quéré, Update on CO_2 emissions, Nat. Geosci. 3 (2010) 811–812.
[4] H. Weigt, D. Ellerman, E. Delarue, CO_2 abatement from renewables in the German electricity sector: Does a CO_2 price help? Energy Econ. 40 (2013) S149–S158.
[5] C. Marcantonini, V. Valero, Renewable energy and CO_2 abatement in Italy, Energy Policy 106 (2017) 600–613.
[6] J. Rockstrom, W. Steffen, K. Noone, A. Persson, F.S. Chapin 3rd, E.F. Lambin, T. M. Lenton, M. Scheffer, C. Folke, H.J. Schellnhuber, B. Nykvist, C.A. de Wit, T. Hughes, S. van der Leeuw, H. Rodhe, S. Sorlin, P.K. Snyder, R. Costanza, U. Svedin, M. Falkenmark, L. Karlberg, R.W. Corell, V.J. Fabry, J. Hansen, B. Walker, D. Liverman, K. Richardson, P. Crutzen, J.A. Foley, A safe operating space for humanity, Nature 461 (2009) 472–475.
[7] N. Armaroli, V. Balzani, The hydrogen issue, ChemSusChem 4 (2011) 21–36.
[8] P.P. Edwards, V.L. Kuznetsov, W.I. David, Hydrogen energy, Philos Trans A Math Phys, Eng Sci 365 (2007) 1043–1056.
[9] H. Zhang, S. Zuo, M. Qiu, S. Wang, Y. Zhang, J. Zhang, X.W.D. Lou, Direct probing of atomically dispersed Ru species over multi-edged TiO_2 for highly efficient photocatalytic hydrogen evolution, Sci Adv 6 (2020).
[10] F. Pellegrino, F. Sordello, L. Mino, C. Minero, V.-D. Hodoroaba, G. Martra, V. Maurino, Formic Acid Photoreforming for Hydrogen Production on Shape-Controlled Anatase TiO_2 Nanoparticles: Assessment of the Role of Fluorides, 101}/{001 Surfaces Ratio, and Platinization, ACS Catal. 9 (2019) 6692–6697.
[11] M.G. Walter, E.L. Warren, J.R. McKone, S.W. Boettcher, Q. Mi, E.A. Santori, N. S. Lewis, Solar water splitting cells, Chem Rev 110 (2010) 6446–6473.
[12] S. Wang, A. Lu, C.J. Zhong, Hydrogen production from water electrolysis: role of catalysts, Nano Converg 8 (2021) 4.
[13] A. Naldoni, M. D'Arienzo, M. Altomare, M. Marelli, R. Scotti, F. Morazzoni, E. Selli, V. Dal Santo, Pt and Au/TiO_2 photocatalysts for methanol reforming: Role of metal nanoparticles in tuning charge trapping properties and photoefficiency, Appl Catal B 130–131 (2013) 239–248.
[14] F. Sordello, F. Pellegrino, M. Prozzi, C. Minero, V. Maurino, Controlled Periodic Illumination Enhances Hydrogen Production by over 50% on Pt/TiO_2, ACS Catal 11 (2021) 6484–6488.
[15] M. Prozzi, F. Sordello, S. Barletta, M. Zangirolami, F. Pellegrino, A. Bianco Prevot, V. Maurino, Assessing a Photocatalytic Activity Index for TiO_2 Colloids by Controlled Periodic Illumination, ACS Catal. 10 (2020) 9612–9623.
[16] Surface chemical analysis — X-ray photoelectron spectrometers — Calibration of energy scales, ISO standard ISO 15472:2010, 2010.
[17] R. Hesse, R. Denecke, Improved Tougaard background calculation by introduction of fittable parameters for the inelastic electron scattering cross-section in the peak fit of photoelectron spectra with UNIFIT 2011, Surf. Interface Anal. 43 (2011) 1514–1526.
[18] P. Agbo, N. Danilovic, An Algorithm for the Extraction of Tafel Slopes, J. Phys. Chem. C 123 (2019) 30252–30264.
[19] P. Quaino, F. Juarez, E. Santos, W. Schmickler, Volcano plots in hydrogen electrocatalysis - uses and abuses, Beilstein J Nanotechnol 5 (2014) 846–854.
[20] A.R. Zeradjanin, J.P. Grote, G. Polymeros, K.J.J. Mayrhofer, A Critical Review on Hydrogen Evolution Electrocatalysis: Re-exploring the Volcano-relationship, Electroanalysis 28 (2016) 2256–2269.
[21] J.K. Nørskov, T. Bligaard, A. Logadottir, J.R. Kitchin, J.G. Chen, S. Pandelov, U. Stimming, Trends in the Exchange Current for Hydrogen Evolution, J. Electrochem. Soc. 152 (2005).
[22] S. Trasatti, Work function, electronegativity, and electrochemical behaviour of metals, J. Electroanal. Chem. Interfacial Electrochem. 39 (1972) 163–184.
[23] J. Qi, J. Resasco, H. Robatjazi, I.B. Alvarez, O. Abdelrahman, P. Dauenhauer, P. Christopher, Dynamic Control of Elementary Step Energetics via Pulsed Illumination Enhances Photocatalysis on Metal Nanoparticles, ACS Energy Lett. 5 (2020) 3518–3525.

[24] Y.M. Psarellis, M.E. Kavousanakis, P.J. Dauenhauer, I.G. Kevrekidis, Writing the Programs of Programmable Catalysis, ACS Catal. 13 (2023) 7457–7471.
[25] M.C. Tavares, S.A.S. Machado, L.H. Mazo, Study of hydrogen evolution reaction in acid medium on Pt microelectrodes, Electrochim. Acta 46 (2001) 4359–4369.
[26] C. Walter, P.W. Menezes, M. Driess, Perspective on intermetallics towards efficient electrocatalytic water-splitting, Chem. Sci. 12 (2021) 8603–8631.
[27] N. Dubouis, A. Grimaud, The hydrogen evolution reaction: from material to interfacial descriptors, Chem. Sci. 10 (2019) 9165–9181.
[28] M.T. Tang, X. Liu, Y. Ji, J.K. Norskov, K. Chan, Modeling Hydrogen Evolution Reaction Kinetics through Explicit Water-Metal Interfaces, J. Phys. Chem. C 124 (2020) 28083–28092.
[29] H. Prats, K. Chan, The determination of the HOR/HER reaction mechanism from experimental kinetic data, Phys. Chem. Chem. Phys. 23 (2021) 27150–27158.